

# Optimal Path-Control for Dual-Frequency Overlay GNSS Receivers

Alexander Rügamer, Cécile Mongrédian, Santiago Urquijo, Günter Rohmer  
Fraunhofer IIS  
Nuremberg, Germany

**Abstract**—This paper presents a general overlay based front-end architecture that enables the joint reception of two signals broadcast in separate frequency bands, sharing just one common baseband stage. The consequences of this overlay in terms of signal quality are analyzed and it is shown that the noise floor superposition results in non-negligible signal degradations. However, it is also demonstrated that these degradations can be minimized by judiciously setting the relative gain between the two signal paths. As an illustration, the analytical optimal path-control expression to combine overlaid signals in an ionospheric-free pseudorange is derived for both Cramér-Rao Lower Bound and practical code tracking parameters.

**Index Terms**—Satellite navigation systems, Global Positioning System, Cramer-Rao bounds, Multiple access interference.

## I. INTRODUCTION

Four different types of satellite navigation services are planned for the European GNSS Galileo: Open Service (OS), Commercial Service (CS), Public Regulated Service (PRS), and Safety-of-Life (SoL). These services are transmitted on independent CDMA (code division multiple access) signals on three frequency bands called E1, E6, and E5, as depicted in Fig. 1. The OS and PRS signals will be available after the launch of the first Galileo IOV satellites in summer/autumn 2011. Both are dual-frequency services transmitted over the E1BC and E5 frequency bands for OS and over the E1A and E6A frequency bands for PRS.

Single-frequency users can receive these services but there are several advantages to multi-frequency processing: The frequency diversity provides a higher robustness against jammers since one signal band may still be usable while the other one is jammed. Moreover a faster reception of the navigation messages is possible since the same information is transmitted on both bands using page swapping [1]. Finally, multi-frequency can be used to form ionospheric-free pseudorange measurements that can remove the first-order ionospheric bias and therefore provide a higher positioning accuracy.

The disadvantage of multi-band reception is a noticeable increase in receiver complexity, size and power consumption, especially for the RF-front-end. In traditional architectures, each additional frequency band to be received requires an extra RF-front-end reception chain.

The complexity of a multi-band RF-front-end can be considerably reduced by sharing front-end components or stages using intentional signal overlay.

Signal overlay is commonly used at the transmitter side: One well-known example is the L1/E1-band centered at

1575.42 MHz which not only provides the GPS L1 C/A, P(Y), M-Code and in the future L1C signals, but also the Galileo E1A and E1BC signals. In addition to these, further signals are/will be transmitted by the Chinese and Russian GNSSs or by the regional SBASs. The sharing of the same frequency band by so many signals is enabled by CDMA multiplex. Several publications investigated the interference and degradations caused by that overlay e.g. [2], [3]. These studies showed that regardless of the congestion, frequency sharing in E1/L1 still works: different signals can coexist thanks to the high spreading rates of the signals and spectral separation provided by the use of different modulations.

This paper follows the same approach but on the receiver side. Specifically it investigates the effects of intentional signal overlay in the analog front-end to validate the combined use of a unique front-end baseband chain and improve the receiver efficiency in terms of cost, size, power consumption, and digital bandwidth.

The general RF-front-end architecture using the overlay principle is presented and illustrated for two frequency combinations: First a dual-frequency E1BC/E5 Galileo OS receiver and then a dual-frequency E1A/E6A Galileo PRS receiver.

For each combination, the overlay-based front-end is optimized in two steps: First, the optimal intermediate frequency is determined to maximize spectral separation and minimize direct signal degradation. Then both signals get overlaid with a controllable relative power between the signal paths. This feature can be used to minimize the signal degradation due to the overlay for a given application. Specifically, the determination of the optimal path control expression to combine overlaid signals in an ionospheric-free pseudorange is investigated with respect to both Cramér-Rao Lower Bound and practical code tracking parameters.

Disclaimer: The PRS is a special Galileo navigation service for governmental and authorized users with controlled access. The PRS information used in the paper is freely available e.g. through the GIOVE-SIS-ICD [4]. No classified documents or information were used.

## II. GALILEO SIGNALS

The power spectral density (PSD) describes the power distribution over the frequency. The PSDs of the Galileo OS and PRS signal components are shown in blue and red, respectively in Fig. 1. Their theoretical expressions, introduced in the following sub-sections, can be used to compute spectral

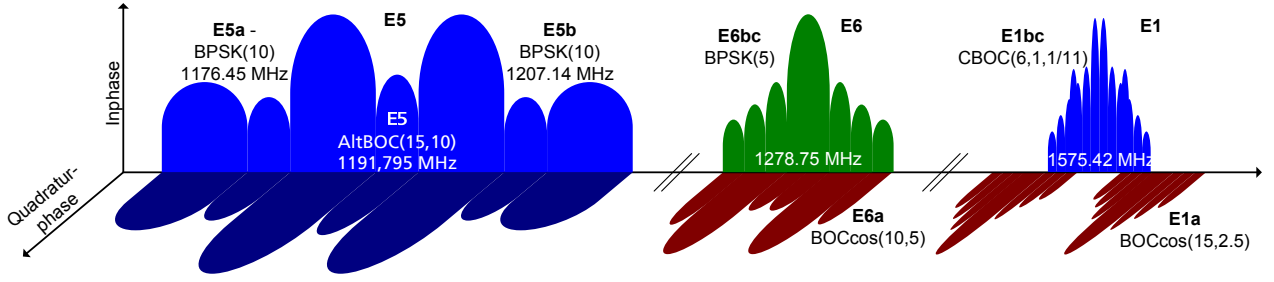


Fig. 1. Galileo Signals

separation coefficients and determine the most appropriate intermediate frequency (IF) for the signal overlay.

#### A. Open Service (OS) PSDs

As depicted in Fig. 1, the Galileo OS signals are transmitted over the E1BC and E5 frequency bands using CBOC(6,1,1/11) and AltBOC(15,10) modulation, respectively.

Suitable reception bandwidths to include all frequency components are approx. 16 MHz and 52 MHz for the E1BC and E5 signals, respectively.

The multiplexed binary offset carrier (MBOC) modulation, implemented as composite BOC (CBOC) for Galileo E1BC is defined in the frequency domain. Specifically, the MBOC PSD is given by

$$S_{\text{CBOC}(6,1,1/11)}(f) = \frac{10}{11}S_{\text{BOCs}(1,1)}(f) + \frac{1}{11}S_{\text{BOCs}(6,1)}(f) \quad (1)$$

using a chipping rate  $f_c$  of 1.023 MHz and sub-carrier rates  $f_s$  of 1.023 MHz and 6.138 MHz for BOCs(1,1) and BOCs(6,1), respectively. The normalized BOCs PSD for even  $2f_s/f_c$  ratio is given in e.g. [5] by

$$S_{\text{BOCs}(f_s, f_c)}(f) = \frac{1}{f_c} \text{sinc}^2\left(\frac{\pi f}{f_c}\right) \tan^2\left(\frac{\pi f}{2f_s}\right). \quad (2)$$

The normalized, analytical, and continuous Galileo E5 AltBOC(15,10) PSD for odd  $2f_s/f_c$  ratio is given by [5]

$$S_{\text{AltBOC}(f_s, f_c)}(f) = \frac{f_c}{2\pi^2 f^2} \cdot \frac{\cos^2\left(\frac{\pi f}{f_c}\right)}{\cos^2\left(\frac{\pi f}{3f_c}\right)} \cdot \left[ \cos^2\left(\frac{\zeta}{2}\right) - \cos\left(\frac{\zeta}{2}\right) - 2 \cos\left(\frac{\zeta}{2}\right) \cos\left(\frac{\zeta}{4}\right) + 2 \right] \quad (3)$$

with  $\zeta = (\pi f)/(f_s)$ ,  $f_s$  being the sub-carrier rate of 15.345 MHz and  $f_c$  being the chipping rate of 10.230 MHz.

#### B. Public Regulated Service (PRS) PSDs

As depicted in Fig. 1, the Galileo PRS signals are transmitted over the E1A and E6A frequency bands, using a BOCc(15,2.5) and BOCc(10,5) modulation, respectively. BOCc uses a cosine phased subcarrier resulting in higher frequency components than with the sine phased subcarrier used in BOCs modulations. As a result, more energy is shifted to the edges of the band. This improves spectral separation with the coexisting OS and CS signals.

Since the BOCc main-lobes are at the edges of the band, the full transmitted bandwidth should be received. According to GIOVE SIS ICD [4] this means a 40.92 MHz bandwidth for E6A and 32.736 MHz for E1A. It should be noted however that the 32.736 MHz bandwidth is not enough to fully include the main-lobes of the E1A BOCc(15,2.5) modulation.

The normalized BOCc PSD for even  $2f_s/f_c$  ratio is also given in [6]:

$$S_{\text{BOCc}(f_s, f_c)}(f) = \frac{4}{f_c} \text{sinc}^2\left(\frac{\pi f}{f_c}\right) \left( \frac{\sin^2\left(\frac{\pi f}{4f_s}\right)}{\cos\left(\frac{\pi f}{2f_s}\right)} \right)^2 \quad (4)$$

### III. DUAL-FREQUENCY GALILEO RECEIVER

The general architecture of a generic dual-band overlay front-end is shown in Fig. 2. The first element is an active multi-band antenna with a first low noise amplifier (LNA) and appropriate bandpass filters (BP). Two analog RF/IF-stages follows, one for each GNSS-band received. The RF/IF-stage consists of an LNA and a bandpass filter with a passband bandwidth of  $BW$ . The mixing stage shifts the RF-signal to an intermediate frequency (IF) where the local oscillator (LO) can be varied. Alternatively the simple mixer can be replaced by an inphase/quadrature phase (I/Q)-demodulator to enable complex IF signal representation.

The combiner overlays both (complex) IF-signals from path 1 and path 2 in the analog domain. Before the overlay, the signals can be amplified or attenuated with a variable gain amplifier (VGA) controllable by the digital signal processing - in most cases the GNSS baseband receiver.

Thanks to this combiner only one common baseband stage, consisting of an anti-aliasing lowpass-filter (LP), automatic gain control (AGC) loop, and the analog-to-digital-converter (ADC), is needed. This allows significant savings in terms of cost, size, power consumption, and digital bandwidth [7].

### IV. SIGNAL OVERLAY DEGRADATION EFFECTS

#### A. Overlay SSC Loss

The spectral separation coefficient (SSC) measures how orthogonal two signals are and can therefore be used to quantify the interference between those signals. If the PSDs do not overlap, e.g. are separated through distant frequency bands, the SSC approaches zero. The PSDs of CBOC, AltBOC and BOCc signals are given in (1) to (4). They are all normalized to unity over infinite bandwidth.

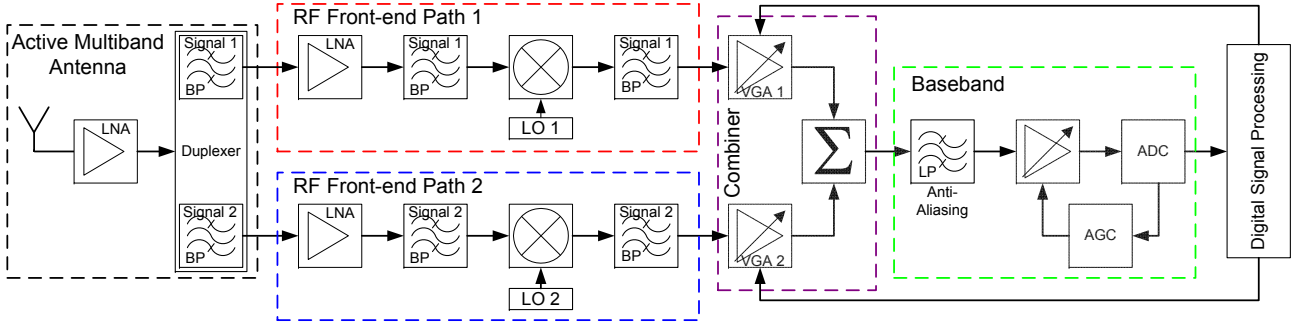


Fig. 2. General Architecture of a Generic Overlay Dual-Frequency GNSS Front-end

The basic SSC equation is given e.g. in [6]. For the case at hand, this equation has to be modified and extended with a frequency shift to account for the fact that the signals use different baseband IFs as well as different bandpass-filters [8]. Thus, the SSC between the desired signal PSD  $S_s$  and the interference signal PSD  $S_i$  is computed as follows

$$SSC = \int_{-\infty}^{\infty} |H_s|^2 S_s(f + f_{IF_s}) |H_i|^2 S_i(f + f_{IF_i}) df \quad (5)$$

with  $|H_{s/i}|$  being the transfer function of an ideal bandpass filter with bandwidth  $BW$ .

In Fig. 3(a) the SSC between the OS signals E1BC CBOC(6,1,1/11) and E5 AltBOC(15,10) was calculated for different receiver bandwidths while the relative intermediate frequency (IF) between these signals was being swept. A local SSC minimum of -87.6 dB/Hz is attained for an IF of 4.4 MHz.

The same approach was used in Fig. 3(b) to find the most appropriate relative IF to overlay the PRS signals E1A BOCc(15,2.5) and E6A BOCc(10,5). In the bandwidth-limited GIOVE-A/B case (green line), the lowest SSC of -103.2 dB/Hz is reached for an IF of 14.7 MHz. The centered overlay spectrum using this relative IF is depicted in Fig. 3(d). It can be seen that the left E1A main-lobe is exactly placed between the two E6A main-lobes providing excellent spectral separation. This IF will be used in the following for the signal overlay between E1A and E6A.

Using these SSC values, the effective  $C/N_{0\text{eff}}$  can be calculated according to [6] with:

$$\frac{C_s}{N_{0\text{eff}}} = \frac{C_s}{N_0} \frac{\int |H_s|^2 S_s(f) df}{\int |H_s|^2 S_s(f) df + \frac{C_i}{N_0} SSC} \quad (6)$$

Since, upon completion of the Galileo FOC, 6 to 11 Galileo satellites are expected to be visible at all time, several interfering signals have to be considered. Doing so, the signal degradation for signal  $S_1$  or signal  $S_2$  can be expressed as

$$\Delta_{SSC\text{-Loss}_{S1/2}} = \frac{C_s/N_0}{C_s/N_{0\text{eff}}} \quad (7)$$

$$= 1 + \sum_{k=1}^N \left[ \frac{C_i}{N_0} \right]_k \frac{SSC_k}{\int |H_s|^2 S_s(f) df} \quad (8)$$

with  $N$  the number of visible Galileo satellites and  $S_2$  the interfering signal for  $S_1$  or vice versa.

Assuming, in a worst case assumption, that 11 Galileo satellites are transmitting with the same power are in view, and that the desired and interfering signals are received with the same  $(C/N_0)$  and without Doppler frequency offset, the losses due to signals overlay remains well below 0.01 dB for  $C_i/N_0$  values ranging between 20 and 45 dBHz. This mainly derives from the low E1BC/E5 and E1A/E6A SSC values obtained when carefully setting the relative IF, as was previously explained and as illustrated in Fig. 3(c) and 3(d), respectively.

### B. Overlay Noise Loss

The aforementioned SSC-loss does not take into account the impact of the additional noise introduced by the combination of the two signal paths. The increased noise-floor (aka. overlay noise) depends on the intersection of the overlaid noise bandwidths (BW) for signals  $S_1$  and  $S_2$  with

$$BW_{\text{Overlay-Noise}_{S1/2}} = \frac{BW_{S1} \cap BW_{S2}}{BW_{S1/2}}. \quad (9)$$

VGA is the relative gain between RF front-end signal path 1 and 2, realized with  $VGA_1$  and  $VGA_2$  settings. The overlay noise loss for signal  $S_1$  and  $S_2$  can then be expressed as

$$\Delta_{\text{Noise-Loss}_{S1}} = 10 \log_{10} \left( 1 + \frac{BW_{\text{Overlay-Noise}_{S1}}}{VGA} \right) \quad (10)$$

and

$$\Delta_{\text{Noise-Loss}_{S2}} = 10 \log_{10} \left( 1 + VGA \cdot BW_{\text{Overlay-Noise}_{S2}} \right). \quad (11)$$

### C. Overall Overlay Loss

Taking into account both signal and noise overlay effects, the  $(C/N_0)_{\text{eff}}$  becomes

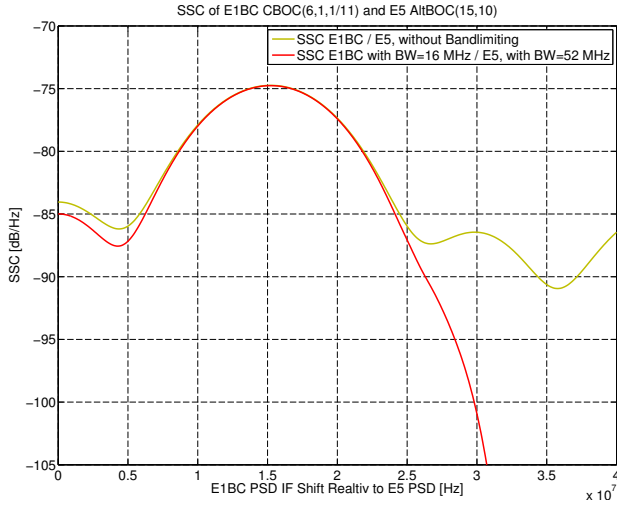
$$\left( \frac{C}{N_0} \right)_{\text{eff}_{S1}} = \left( \frac{C}{N_0} \right)_{S1} - \Delta_{SSC\text{-Loss}_{S1}} - \Delta_{\text{Noise-Loss}_{S1}} \quad (12)$$

$$\approx \frac{(C/N_0)_{S1}}{1 + \frac{1}{VGA} \cdot BW_{\text{Overlay-Noise}}} \quad (13)$$

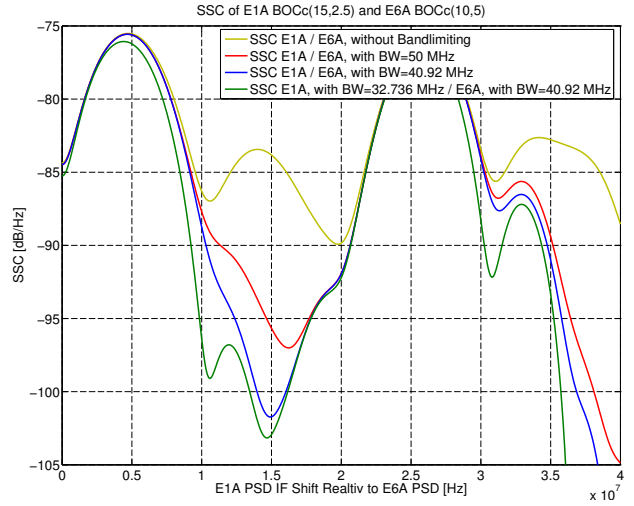
and

$$\left( \frac{C}{N_0} \right)_{\text{eff}_{S2}} = \left( \frac{C}{N_0} \right)_{S2} - \Delta_{SSC\text{-Loss}_{S2}} - \Delta_{\text{Noise-Loss}_{S2}} \quad (14)$$

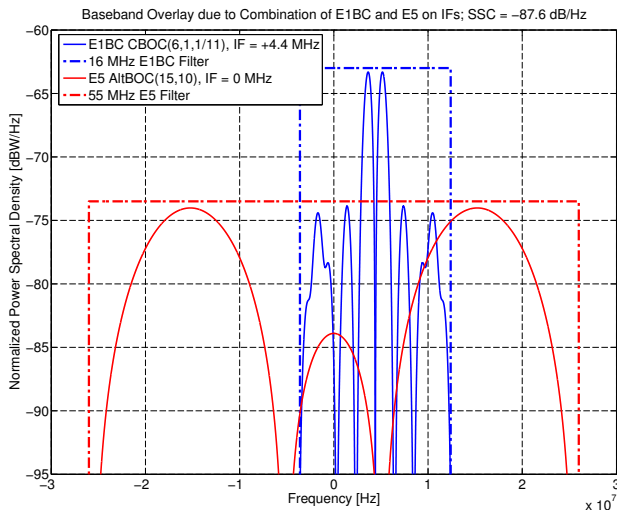
$$\approx \frac{(C/N_0)_{S2}}{1 + VGA \cdot BW_{\text{Overlay-Noise}}}. \quad (15)$$



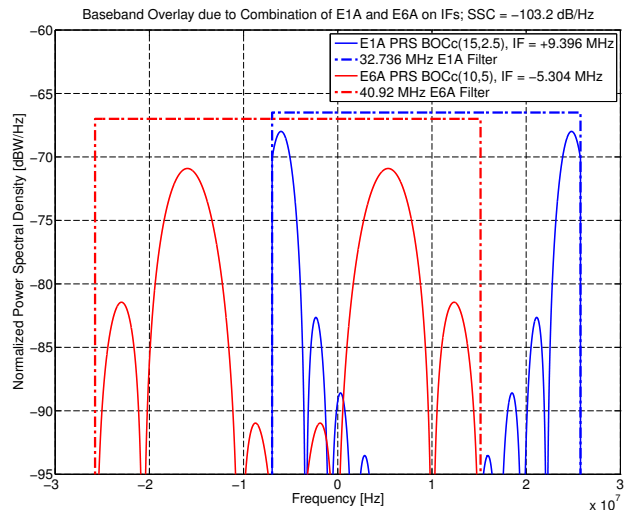
(a) SSC for Different IFs between the OS Signals E1BC and E5



(b) SSC for Different IFs between the PRS Signals E1A and E6A



(c) Galileo OS Signal Overlay E1BC with E5 on IF



(d) Galileo PRS Signal Overlay E1A with E6A on IF

Fig. 3. SSC and Spectral Overlay on different IFs for OS and PRS Dual-Frequency Examples

for signal  $S_1$  and  $S_2$ , respectively and where  $\Delta_{\text{SSC-Loss}_{S1/2}}$  was previously shown to be negligible.

## V. TRACKING AND MEASUREMENT ACCURACY IN OVERLAY RECEIVERS

### A. CRLB Code Tracking Error

To analyze the impact of thermal noise on the code tracking accuracy regardless of most receiver-dependent tracking settings, it is useful to calculate the Cramér-Rao Lower Bound (CRLB) [9] given by

$$\sigma_{\text{crlb}}^2 = (c_0)^2 \frac{B_L}{(2\pi)^2 (C/N_0)_{\text{eff}} \beta_{\text{rms}}^2} \quad (16)$$

where  $c_0$  is the speed of light,  $B_L$  is the code loop bandwidth and

$$\beta_{\text{rms}}^2 = \int_{+BW/2}^{-BW/2} f^2 S(f) df \quad (17)$$

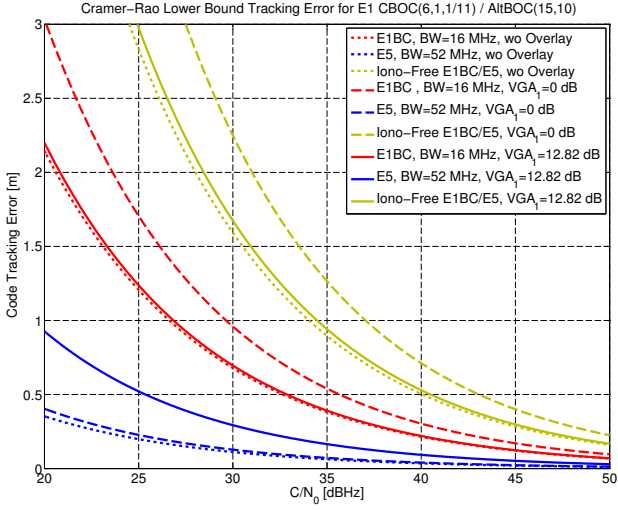
is the root-mean-square bandwidth of the signal.

The equivalent CRLB code tracking error in meter with a code loop bandwidth of 1 Hz is plotted in dotted lines in Fig. 4(a) and 4(b) for the OS and PRS signals, respectively.

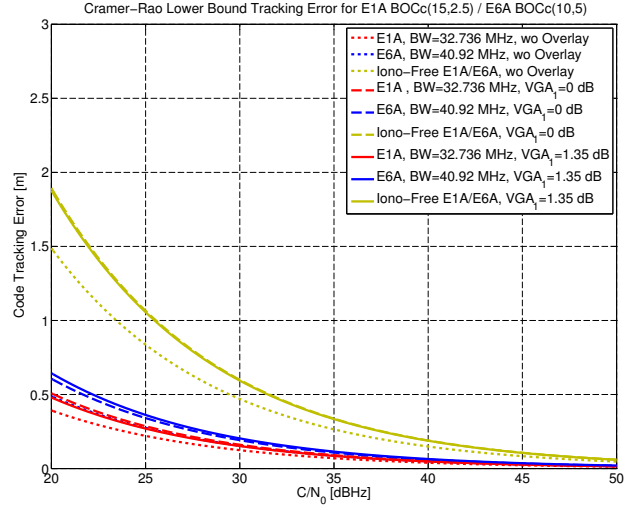
### B. Ionosphere-Free Tracking Error

One of the main advantage of multi-band GNSS reception is that it enables direct observation and almost complete elimination of the ionosphere-induced ranging bias. Because the ionosphere is a dispersive medium, the magnitude of the group delay (or, equivalently ranging bias) experienced by signals broadcast by a unique satellite but at different frequencies will differ. This allows the dual- or multi-frequency users to form the so-called ionosphere-free pseudorange measurements,  $\rho_{IF}$ , according to the following Equation, cf. [9]:

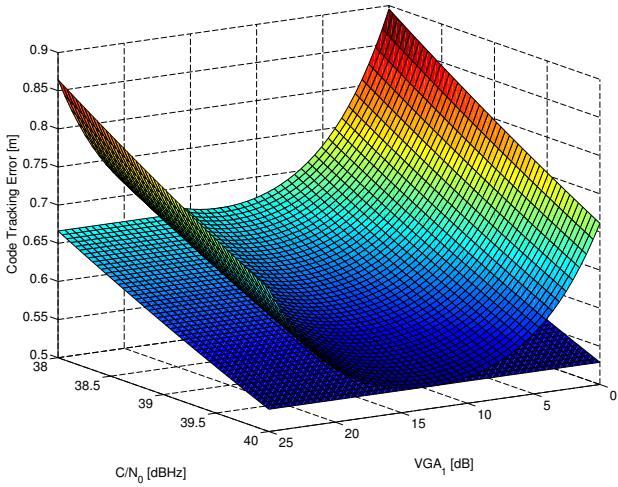
$$\rho_{IF} = \frac{\gamma}{\gamma - 1} (\rho_{f1} + \sigma_{f1}) - \frac{1}{\gamma - 1} (\rho_{f2} + \sigma_{f2}) \quad (18)$$



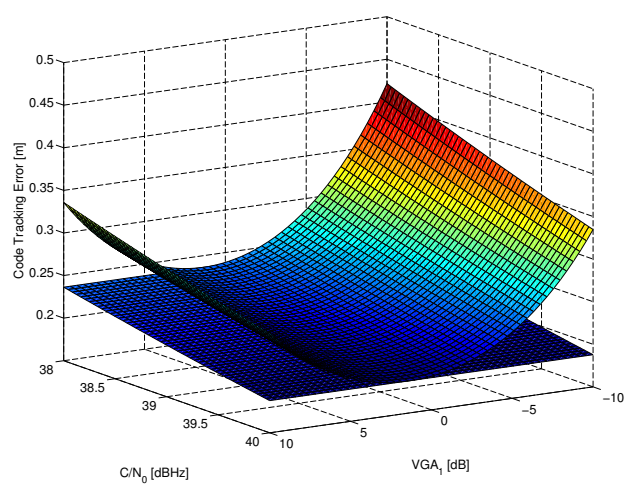
(a) CRLB Code Tracking Error for E1BC CBOC(6,1,1/11), E5 Alt-BOC(15,10) and IF-linear-Combination with Different VGA Settings



(b) CRLB Code Tracking Error for E1A BOCcos(15,2.5) with E6A BOCcos(10,5) and IF-linear-Combination with Different VGA Settings



(c) E1BC / E5 IF Code Tracking Error vs. VGA Settings and  $C/N_0$



(d) E1A / E6A IF Code Tracking Error vs. VGA Settings and  $C/N_0$

Fig. 4. Code Tracking Error for CRLB and Ionospheric-Free Linear Combination Tracking in Dependency of the VGA Setting

with  $\gamma = (f_1/f_2)^2 > 1$ , where  $\rho_{f_{1/2}}$  are the pseudorange measurements for  $S_1$  and  $S_2$ , respectively and  $\sigma_{f_{1/2}}$  is the pseudorange noise of these signals. Ignoring the contribution of multipath, the pseudorange noise is the direct translation of the code jitter into the measurement domain.

For an OS-Galileo dual-band receiver

$$\gamma_{OS} = \frac{f_{E1}}{f_{E5}} = \frac{1575.42 \text{ MHz}}{1191.795 \text{ MHz}} \approx 1.75 \quad (19)$$

and for the PRS-Galileo dual-band-receiver

$$\gamma_{PRS} = \frac{f_{E1}}{f_{E6}} = \frac{1575.42 \text{ MHz}}{1278.75 \text{ MHz}} \approx 1.52. \quad (20)$$

Looking at (18) again, it can be seen that the removal of the ionosphere-induced ranging bias comes at the expense of a noise increase. The magnitude of this noise increase depends on the single frequency pseudorange noises and on the relative frequency spacing of the two signals used to form the ionosphere-free measurement.

More specifically, it is possible to compute  $\sigma_{IF}$ , the ionosphere-free pseudorange noise, according to the following Equation:

$$\sigma_{IF} = \sqrt{\frac{\gamma^2}{(\gamma-1)^2} \cdot \sigma_{f1}^2 + \frac{1}{(\gamma-1)^2} \cdot \sigma_{f2}^2} \quad (21)$$

The higher frequency pseudorange error  $\sigma_{f1}^2$  (e.g. E1) has always more effect on the overall ionosphere-free pseudorange than the lower one  $\sigma_{f2}^2$  (e.g. E5 or E6).

When the signals are overlaid as shown in Fig. 3(c) and 3(d) with  $VGA = 0 \text{ dB}$  the effective  $(C/N_0)_{\text{eff}}$  can be calculated for signals  $S_1$  and  $S_2$  with (13) and (15), respectively. The equivalent CRLB code tracking error in meter for signal overlay is plotted in dashed lines in Fig. 4(a) and 4(b). It can be noted that, as expected, the CRLB is lower when no overlay is used.

### C. Optimal VGA-Control for CRLB IF-Tracking

According to (16) the pseudorange error  $\sigma_{crlb}^2$  directly depends on the  $(C/N_0)_{\text{eff}}$  which, in turns, directly depends on the relative VGA setting between the signal path 1 and 2. The surfaces in Fig. 4(c) and 4(d) show the CRLB ionosphere-free code tracking error  $\sigma_{\text{IF}}$  in meter for different VGA settings. The intersecting plane shows the minimum reachable error.

Thanks to the additional degree of freedom given with the path-control, the VGA can be set to an optimized value for low  $\sigma_{\text{IF}}$  for dual-frequency ionosphere-free pseudorange measurements.

Combining (13), (15), (16) in (21), it is possible to express the  $\sigma_{\text{IF}}$  tracking variance as a function of the VGA setting. One can then find the VGA setting that minimizes the  $\sigma_{\text{IF}}$  tracking variance by deriving this expression with respect to VGA and setting it to zero:

$$\frac{\partial \sigma_{\text{IF}}(\text{VGA})}{\partial \text{VGA}} = 0 \quad (22)$$

Doing so, the optimal VGA setting can be expressed as:

$$\text{VGA}_{\text{opt}} = \left( \frac{f_1}{f_2} \right)^2 \frac{\beta_{\text{rms}2}}{\beta_{\text{rms}1}} \sqrt{\frac{BW_2 B_{L1} C/N_{02}}{BW_1 B_{L2} C/N_{01}}} \quad (23)$$

For the E1BC/E5 OS ionosphere-free combination the optimal VGA setting is 12.82 dB. The resulting CRLB- $\sigma_{\text{IF}}$ -code tracking error is plotted with the continuous line in Fig. 4(a) and demonstrates that in order to improve the E1BC/E5 OS ionosphere-free pseudorange measurement accuracy it is beneficial to release the E1 path from "E5-noise". With this optimized VGA setting, the error tends toward the theoretical CRLB error without overlay (that is, if two separate RF-front-ends were used).

For the E1A/E6A PRS ionosphere-free combination the optimal VGA setting is 1.35 dB showing that the case without any VGA control already approaches the theoretical CRLB error without overlay. Even though the benefits brought by active VGA control is less significant for PRS signals than it was for OS signals, Fig. 4(d) clearly shows that care should be taken to set the relative amplification of the overlaid signal paths to an appropriate value.

### D. Optimal VGA-Control for Practical Iono-Free Tracking

Assuming that the signal is received with an infinite front-end bandwidth and that the Delay-Lock Loop (DLL) uses a Dot-Product (DP) discriminator, [10] showed that the  $1-\sigma$  code tracking error due to additive white Gaussian noise can be approximated by:

$$\sigma_{\text{dll}}^2 = \frac{c_0^2}{f_c^2} \cdot \frac{B_L(1 - B_L T/2)\delta}{2 C/N_0 \alpha} \cdot \left( 1 + \frac{1}{T C/N_0} \right) \quad (24)$$

where  $f_c$  is the received signal's chipping rate,  $T$  is the coherent integration time used,  $\delta$  is the early-late spacing, and  $\alpha$  corresponds to the slope of the auto-correlation main peak.

Neglecting the squaring loss (the brackets in (24)), the optimal VGA settings can be derived in the same way as before. Thus the approximately optimal VGA setting for

iono-free linear combination in DLL-code tracking loops is expressed as

$$\text{VGA}_{\text{opt-dll}} = \left( \frac{f_1}{f_2} \right)^2 \frac{f_{c2}}{f_{c1}} \sqrt{\frac{BW_2 C/N_{02}}{BW_1 C/N_{01}}} \cdot \sqrt{\frac{\alpha_1 B_{L1}(1 - B_{L1} T_1/2)\delta_1}{\alpha_2 B_{L2}(1 - B_{L2} T_2/2)\delta_2}} \quad (25)$$

## VI. CONCLUSION

A general overlay based front-end architecture that enables the joint reception of two signals broadcast in separate frequency bands, sharing just one common LP/AGC/ADC baseband stage was presented. The signal degradation effects due to the overlay were analyzed and it was concluded that signal superposition has a negligible impact on signal quality but not noise-floor superposition. However, the degradation resulting from the noise-floor combination can be minimized by setting the relative gain between the two signal paths to an appropriate value. The analytical optimal path-control expression was derived for both Cramér-Rao Lower Bound and practical code tracking parameters in an ionospheric-free linear combination using overlaid signals.

For future work the theoretical results presented here regarding the benefits of path control VGA in terms of tracking accuracy and dual-frequency ionospheric correction efficiency will be confirmed in a hardware demonstrator setup.

## REFERENCES

- [1] "European GNSS (Galileo) Open Service Signal In Space Interface Control Document (OS SIS ICD) Issue 1," European Union/European GNSS Supervisory Authority (GSA), Tech. Rep., February 2010.
- [2] S. Wallner, G. W. Hein, T. Pany, J.-A. Avila-Rodriguez, and A. Posfay, "Interference Computations Between GPS and GALILEO," in *Proceedings of the 18th International Technical Meeting of the Satellite Division of The Institute of Navigation (ION GNSS 2005)*, Long Beach, CA, September 2005, pp. 861-876., 2005.
- [3] W. Liu, S. Li, L. Liu, M. Niu, and X. Zhan, "A Comprehensive Methodology for Assessing Radio Frequency Compatibility for GPS, Galileo and Compass," in *Proceedings of the 23th International Technical Meeting of the Satellite Division of The Institute of Navigation, ION GNSS 2010*, Portland, Oregon, September 20-24, 2010.
- [4] "GIOVE-A + B (#102) Navigation Signal-in-Space Interface Control Document (GIOVE-A+B Public SIS ICD), ESA-DTEN-NG-ICD/02837," ESA ESTEC, Tech. Rep., 2008.
- [5] E. Rebeyrol, C. Macabiau, L. Lestarquit, L. Riesa, J.-L. Issler, M.-L. Boucheret, and M. Bousquet, "BOC power spectrum densities," in *Proceedings of the 2005 National Technical Meeting of The Institute of Navigation, San Diego, CA, January 2005*, pp. 769-778., 2005.
- [6] E. D. Kaplan and C. J. Hegarty, *Understanding GPS: Principles and Applications, Second Edition*. Artech House, 2006.
- [7] A. Ruegamer, S. Urquijo, and G. Rohmer, "Multi-band GNSS Front-end Architecture Suitable for Integrated Circuits," in *Proceedings of the 2010 International Technical Meeting of The Institute of Navigation, San Diego, CA, January 2010*, pp. 688-697., 2010.
- [8] A. Ruegamer, C. Mongredien, S. Urquijo, and G. Rohmer, "A Novel Overlay-Architecture Based GNSS Multi-Band Front-End," in *Proceedings of the 2010 European Navigation Conference, ENC GNSS 2010, Braunschweig, Germany, Oct. 19 - 21, 2010*, 2010.
- [9] U. Engel, "Improving position accuracy by combined processing of Galileo and GPS satellite signals," in *Information Fusion, 2008 11th International Conference on*, 2008, pp. 1 - 8.
- [10] O. Julien, "Design of Galileo L1F Receiver Tracking Loops," Ph.D. dissertation, UCGE Report No. 20227, The University of Calgary, Department of Geomatics Engineering, 2005.